



# Comparison of Kinetics, Oxide Crystal Growth and Diffusivities of Nano- and Micrometer-Sized Copper Particles on Oxidation in Air



Norbert Eisenreich, Olga Schulz, Andreas Koleczko, Sebastian Knapp\*

Fraunhofer Institut für Chemische Technologie ICT, Joseph-von-Fraunhofer-Str, 7, D-76327 Pfinztal, Germany

## ARTICLE INFO

**Keywords:**  
oxidation  
copper particles  
kinetics  
diffusion  
crystallite growth

## ABSTRACT

The oxidation of nanometer-sized and micrometer-sized copper particles with diameters of 60 nm and 20  $\mu\text{m}$  is investigated in air in the temperature range from 323 to 1273 K, using high-temperature X-ray diffraction and thermal analysis with multiple heating rates. The oxidation of both particle types occurs in two steps to  $\text{Cu}_2\text{O}$  and to  $\text{CuO}$  in a similar way, the nanometer-sized particles at substantially lower temperatures and the two steps separated. The kinetics are investigated for both steps using a least squares fit procedure, comparing three different mechanisms: consecutive reaction steps of 1st order, step one with 1st order followed by a step modeled with Shrinking Core (SC) model and two steps connected with two SC models. The diffusivities with lowest standard deviations are:  $\text{Log}_{10}(Z_{1d}) = -5.234 \text{ cm}^2 \text{ s}^{-1}$ ,  $E_1 = 88.5 \text{ kJ/mol}$ , and  $\text{Log}_{10}(Z_{2d}) = -3.873 \text{ cm}^2 \text{ s}^{-1}$ ,  $E_2 = 122.7 \text{ kJ/mol}$  from the X-ray study for the 20  $\mu\text{m}$  particles. For the 60 nm particles  $\text{Log}_{10}(Z_1) = 8.08 \text{ s}^{-1}$  (1st order reaction),  $E_1 = 89.15 \text{ kJ/mol}$  and  $\text{Log}_{10}(Z_{2d}) = -5.09 \text{ cm}^2 \text{ s}^{-1}$  (diffusion),  $E_2 = 107.4 \text{ kJ/mol}$  are found. These values are within the range of those obtained from copper plates. The crystallite size of the oxide particles begins at about 3–10 nm to be evaluated. It increases on temperature rise to be described by a nucleation mechanism, the kinetics being evaluated.

## 1. Introduction

Copper and its oxides have strong impact on many industrial branches, including metallurgy, electrochemistry, electronics, catalysis, energy storage, energy conversion, safety with corrosion [1], which is an important issue. Research and applications of copper and copper oxide nanoparticles spread out extensively to many areas [2] for example to semiconductors [3], microbiology [4], catalysis [5], energy storage [6–9], energetic materials [10–15] and many others. Some papers consider especially the oxidation behavior.

The copper oxidation, comprising the steps to  $\text{Cu}_2\text{O}$  and to  $\text{CuO}$ , was extensively studied for flat plates and thin films inducing 1-dimensional geometry (see e.g. Ref. [15–18]). For thick oxide layers on the surface, parabolic rate laws were found caused by a rate-controlling diffusion (Jander equation) [15–17,19]. This diffusion of the metal through the oxide layer to the surface and the subsequent oxidation was shown

already in the past [20]. As a consequence, hollow oxide particles are formed from particles at the oxidation process [21–23]. Thin oxide layers may exhibit logarithmic rate laws according to the Cabrera-Mott mechanisms [16]. However, the oxidation of copper particles requires further investigation, especially when including nanometer-sized particles.

Particles with sizes smaller than 100 nm show superior surface-volume ratios and growing influence of initial oxide layers, which are present if exposed to air. The linear diffusion models [16,19] for plates have to be substituted by models of spherical symmetry, e.g. 3D-Jander Equation or the Shrinking Core (SC) model [15,24,25]. In this paper, the results of oxidation of nanometer-sized and micrometer-sized copper particles by thermogravimetry (TG) and by X-ray diffraction measurements are presented and the kinetic mechanisms and parameters analyzed. It uses parts of a doctoral thesis [15] with further work.

**Abbreviations:** BET, Brunauer, Emmett and Teller method; DTG, differential thermogravimetry; FE-SEM, field emission scanning electron microscopy; SC, shrinking core (model); TG, thermogravimetry;  $E_i(x)$ , exponential integral;  $c$ , conversion factor;  $c_{\text{O}_2}$ , oxygen concentration in  $\text{mol/m}^3$ ;  $D(T)$ , diffusivity in  $\text{cm}^2/\text{s}$ ;  $E$ , activation energy in  $\text{J/mol}$ ;  $n$ , exponent;  $k(T)$ , reaction rate in  $1/\text{s}$ ;  $M$ , molar mass in  $\text{kg/mol}$ ;  $M_{\text{Cu}}$ , molar mass of copper 63.546  $\text{g/mol}$ ;  $p$ , conversion factor relates normalized to measured data;  $R$ , ideal gas constant 8.3144598  $\text{J/(mol K)}$ ;  $r_c$ , radius of metal core in  $\text{m}$ ;  $R_s$ , surface radius in  $\text{m}$ ;  $T$ , temperature in  $\text{K}$ ;  $f(x)$ , reaction mechanism;  $g(x)$ , integrated reaction mechanism;  $u(T)$ , conversion of  $\text{Cu}$ ;  $v$ , normalized volume (dimensionless); 1, 2, subscripts for  $\text{Cu}_2\text{O}$  or  $\text{CuO}$ , respectively;  $tg$ ,  $sc$ , subscripts for model 1st order or SC model;  $i, j$ , subscripts for single data points:  $i$  - of curve,  $j$  - heating rate;  $N_j$ , number of data points of curve with heating rate  $j$ ;  $x(T)$ , conversion of initial species;  $y(T)$ , conversion of intermediate species for  $\text{Cu}_2\text{O}$ ;  $z(T)$ , conversion of final species for  $\text{CuO}$ ;  $\chi^2$ , squared differences of measured data to calculated ones;  $Z$ , pre-exponential factor of the reaction coefficient in  $1/\text{s}$ ;  $Z_d$ , pre-exponential factor of the diffusion coefficient in  $\text{cm}^2/\text{s}$ ;  $\beta$ , heating rate in  $\text{K/min}$ ;  $\rho_{\text{Cu}}$ , density of copper 8960  $\text{kg/m}^3$ ;  $\sigma$ , relative standard deviation (dimensionless)

\* Corresponding author.

E-mail address: [sebastian.knapp@ict.fraunhofer.de](mailto:sebastian.knapp@ict.fraunhofer.de) (S. Knapp).

<http://dx.doi.org/10.1016/j.tca.2017.05.012>

Received 1 February 2017; Received in revised form 11 May 2017; Accepted 13 May 2017

Available online 15 May 2017

0040-6031/ © 2017 Elsevier B.V. All rights reserved.

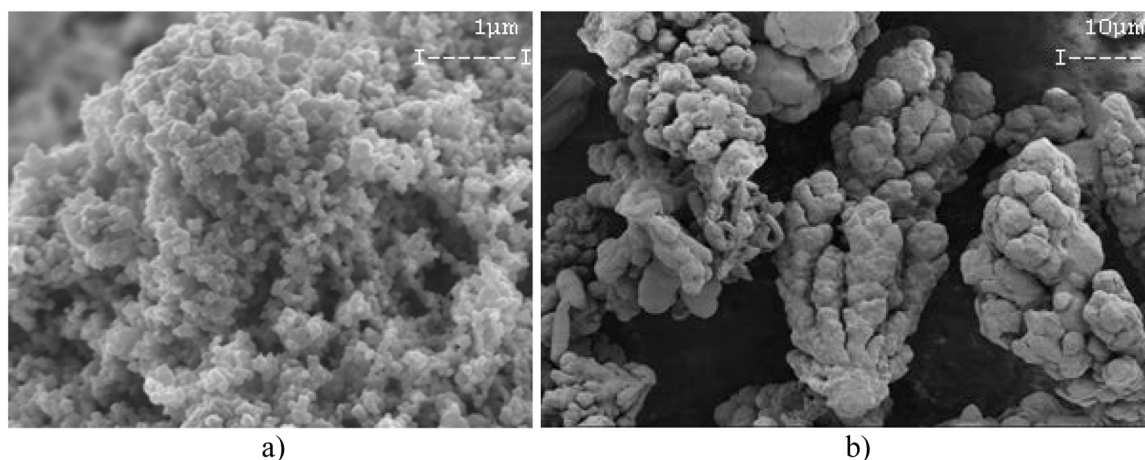


Fig. 1. FE-SEM-images of Cu particles (a) particles of Cu-1 sample and (b) particles of Cu-2 sample at room temperature.

## 2. Experimental

The nanometer-sized (0.06  $\mu\text{m}$ ) and micrometer-sized (10  $\mu\text{m}$ ) Cu particles were supplied by SIBTHERMOCHIM, Russia (particle supplier) [10], obtained by wire explosion. The size and morphology of the particles were analyzed by field emission scanning electron microscopy (FE-SEM) using a SUPRA 55 VP, Carl Zeiss SMT AG, Germany (Fig. 1). The specific surfaces were measured by gas sorption with a Quantachrome Nova 2000e, Quantachrome Instruments, USA. The results are listed in Table 1.

The nanometer-sized particles show a nearly spherical shape and had loosely agglomerated, but they still showed a specific surface of 7.1  $\text{m}^2/\text{g}$  which corresponds to even a smaller diameter (see Table 1). On exposure to air the small particles started immediately to react with glowing and changing colors, rapidly. The larger particles with a surface area of 0.2  $\text{m}^2/\text{g}$  have diameters of 10  $\mu\text{m}$  to 20  $\mu\text{m}$  and show a substructure of about 1–2  $\mu\text{m}$ , which more or less corresponds to the surface area obtained by the gas absorption method. The shapes might average to spherical shape. On oxidation, the particles partially agglomerate in porous hollow structure partially with whiskers [15,26,27]. In Ref [15] pre-oxidized Cu-1 samples were mainly described. The impurities listed in Table 1 are small and are assumed not to catalyze the oxidation.

The crystalline phases, formed during oxidation, were determined by in-situ high-temperature X-ray diffraction (Cu  $K_{\alpha 1}$ ,  $\lambda = 154.0598$  pm) using a Bruker AXS D8 diffractometer, USA, with a high temperature cell. All oxidation experiments were performed in air. Diffraction patterns of the Cu-2 particles were taken at  $2\theta$  ranging from  $20^\circ$  to  $80^\circ$ . During the temperature-controlled experiments, samples were heated up in steps of 25 K from 323 K to 1273 K. At each step, the temperature was hold for two hours and diffraction patterns were taken with a scan rate of 0.05  $^\circ/\text{s}$ . The heating rate from one temperature level to the next one was 1 K/s. This corresponds to an effective heating rate of 0.21 K/min. Cu-1 particles were scanned from  $30^\circ$  to  $60^\circ$  after one hour of constant temperature, heated up in steps of 5 K which corresponds to a heating rate of 0.43 K/min. The diffraction patterns were evaluated using the TOPAS software of Bruker AXS which give relative intensities, concentrations and crystallite sizes versus temperature. However, the

data scatter substantially at low peak intensities. The peaks were also analyzed by a difference method [28], which is more sensitive for small peaks and noisy X-ray diagrams, as obtained for the Cu-1 particles. It uses a part of the diagrams including one or more peaks of one species. The resulting curves are compared to the thermo-analytical curves. The non-isothermal thermogravimetric analysis (TG) was carried out with heating rates of 2 K/min, 5 K/min and, 10 K/min up to 1473 K (Netzsch STA 449C Jupiter, Netzsch GmbH & Co. Holding KG, Germany).

The kinetic evaluation of the TG and X-ray data utilized three models: a reaction step of 1st order, followed by a further 1st order one, or followed by a SC-model or two subsequent SC-models. A least squares fit procedure used the Routine “FindMinimum” of Mathematica<sup>®</sup> by Wolfram Research Inc., USA.

## 3. Results and discussion

### 3.1. Non-isothermal oxidation behavior by TG/DTG

The oxidation of the nanometer-sized sample (Cu-1) occurs in two stages as indicated by two consecutive sigmoid curves for the reaction  $4\text{Cu} + 2\text{O}_2 \rightarrow 2\text{Cu}_2\text{O} + \text{O}_2 \rightarrow 4\text{CuO}$  even more indicated by the two peaks of the DTG curve (Fig. 2a). The maxima are at 444 K and at 565 K (5 K/min, Fig. 2) other heating rates shift the curves to higher and lower temperatures. The mass increase after the steep rise (above 620 K) is assigned to the oxidation of some larger particles in the powder and is not considered in the further evaluation. The final mass increase of Cu-1 reaches about 24.1 % at 1273 K compared to 25.2 % of a complete oxidation. It corresponds to the purity listed in Table 1. Cu-2 shows a mass increase on oxidation, which is nearly linear (Fig. 2). Its DTG curve consists of an initial peak and proceeds with a plateau between 560 and 850 K. The final mass gain of these particles reaches 24.6 %. Similar curves like for Cu-1 of Fig. 2a were analyzed earlier by other models [15,29–31], or for TiN oxidation with successive reaction steps by Jander 3-D models. [32]

### 3.2. Identification of oxidation products and phase transformation

In Fig. 3, diffraction diagrams of the particles are presented. For Cu-

Table 1

Characteristics of the nanometer- and micrometer-sized copper particles, gas absorption measurements indicates the big particles being composed of smaller ones.

Sample	Diameter FE-SEM	purity (each: Au, C, Al < 0.1)	BET surface	Diameter correlated to BET	Estimated (TG) $\text{Cu}_2\text{O}$	Estimated (TG) CuO
Dim.	[ $\mu\text{m}$ ]	[%]	[ $\text{m}^2/\text{g}$ ]	[ $\mu\text{m}$ ]	[%]	[%]
Cu-1	0.06	96.3	7.1	0.047	1.8	1.9
Cu-2	20	99.8	0.2	1.68	Not detected	Not detected

Download English Version:

<https://daneshyari.com/en/article/4995944>

Download Persian Version:

<https://daneshyari.com/article/4995944>

[Daneshyari.com](https://daneshyari.com)